Optimal tuning of solid-state quantum gates: A universal two-qubit gate

E. Paladino,[1,2] A. Mastellone,[3,1,2] A. D'Arrigo,[1,2] and G. Falci[1,2]

[1]*Dipartimento di Metodologie Fisiche e Chimiche (DMFCI), Università di Catania, Viale A. Doria 6, 95125 Catania, Italy*
[2]*MATIS CNR-INFM, Catania, Italy*
[3]*Centro Italiano Ricerche Aerospaziali (CIRA), Via Maiorise snc, Capua, 81043 Caserta, Italy*

We present a general route to reduce inhomogeneous broadening in nanodevices due to $1/f$ noise. We apply this method to a universal two-qubit gate and demonstrate that for selected *optimal couplings*, a high-efficient gate can be implemented even in the presence of $1/f$ noise. Entanglement degradation due to interplay of $1/f$ and quantum noise is quantified via the concurrence. A charge-phase $\sqrt{i-\mathrm{SWAP}}$ gate for spectra extrapolated from single-qubit experiments is analyzed.

Intense research on solid-state nanodevices during the last decade lead to observation of fundamental quantum phenomena at the nanoscale. Combining quantum coherence with the existing integrated-circuit fabrication technology makes nanocircuits very promising for quantum computing. In particular, a variety of high-fidelity single-qubit gates on a superconducting platform are nowadays available.[1–3] Controlled generation of entangled states and preserving quantum correlations represent a timely and critical issue. Identification of strategies to counteract physical processes detrimental to quantum coherent behavior is a fundamental step toward this goal.

Noise with $1/f$ spectrum is ubiquitous in nanodevices and represents a serious limitation for their coherence properties.[1–6] Because of low-frequency fluctuations of the device eigenenergies, the average (implied by quantum measurement) of signals occurring at slightly different frequencies, is defocused. This effect, analogous to inhomogeneous broadening,[7] is a signature of $1/f$ noise, whatever its microscopic origin. It results in a typical algebraic decay of coherent oscillations,[8] as observed in single-qubit gates of various design and materials.[2,3]

One way to defeat inhomogeneities is exploiting NMR decoupling procedures.[9] For instance, echo-type protocols may considerably reduce defocusing in single-qubit rotations,[2,5,10] but they also limit external control on quantum state processing. Moreover, extension to multiqubit gates may require a large fraction of quantum operations devoted to effective decoupling procedures, limiting scalability. A simpler but effective strategy is to operate the device at "optimal points," characterized by minimal sensitivity of the relevant splittings to variations in the control parameters. Partial reduction in defocusing of single-qubit operations by operating at such working point has been successfully demonstrated.[1,2,10]

In this Brief Report, we extend this scheme and present a general route to reduce inhomogeneous broadening effects in nanodevices. The strategy we propose exploits tunability to counteract the effect of noise channels opened up by control parameters themselves. Beside the interest for quantum gates engineering, on a more fundamental level our analysis is relevant for optimizing fault-tolerant architectures,[11] showing that the influence of $1/f$ fluctuations in the solid state can be limited by exploiting the band structure of coupled nanodevices.

We apply this method to a universal two-qubit gate involving an entanglement operation on two quantum bits, a necessary step toward the construction of a scalable quantum computer.[12] We consider a $\sqrt{i-\mathrm{SWAP}}$ gate based on a fixed coupling scheme and show that, for selected *optimal couplings*, it can be accurately operated even in the presence of $1/f$ and high-frequency noise. As a relevant example, we analyze a realistic charge-phase two-qubit gate.[13]

Optimal tuning. We denote the device Hamiltonian with $\mathcal{H}_0$, and its eigenvalues as ω_i. Fluctuations of the control parameters due to external environments are modeled by $\mathcal{H}_I = -\frac{1}{2}\Sigma_\alpha \hat{Q}_\alpha \otimes \hat{X}_\alpha$. Here, $\{\hat{X}_\alpha\}$ are collective environmental variables coupled to the nanodevice operators, $\hat{Q}_\alpha$. Typically, power spectra of $\hat{X}_\alpha$ display a $1/f$ low-frequency behavior up to some cutoff, followed by a white or ohmic flank.[2,14] Defocusing is due to low-frequency fluctuations whereas noise at high frequencies (on the order of the eigensplittings) is responsible for system-bath inelastic energy exchanges. Acting on different time scales, these two processes can be considered separately. Upon extending the multistage elimination approach,[8] we separate the effects of low- and high-frequency components of the noise by setting $\hat{X}_\alpha \rightarrow X_\alpha(t) + \hat{X}_\alpha^f$. Here, $\{X_\alpha(t)\} = \mathbf{X}(t)$ are classical stochastic variables describing low-frequency ($1/f$) noise, and can be treated in the adiabatic approximation (adiabatic noise). Instead, high-frequency fluctuations $\hat{X}_a^f$ are modeled by a Markovian bath and mainly determine spontaneous decay (quantum noise). Nanodevice populations relax due to quantum noise (T_1-type times), which also leads to secular dephasing ($T_2^* = 2T_1$ type). Defocusing due to low-frequency noise determines further decay of the coherences.

In the adiabatic and longitudinal approximation[8] the system evolution is related to instantaneous eigenvalues, $\omega_i[\mathbf{X}(t)]$, which depend on the noise realization. The leading effect of low-frequency fluctuations in repeated measurements is given within the static path approximation (SPA). It amounts to replace, in the path-integral average over $\mathbf{X}(t)$ realizations, $X_\alpha(t)$ with statistically distributed values $X_\alpha(0) \equiv X_\alpha$ at each repetition of the measurement protocol. As a consequence, level splittings $\omega_{ij}(\mathbf{X})$ are random variables,
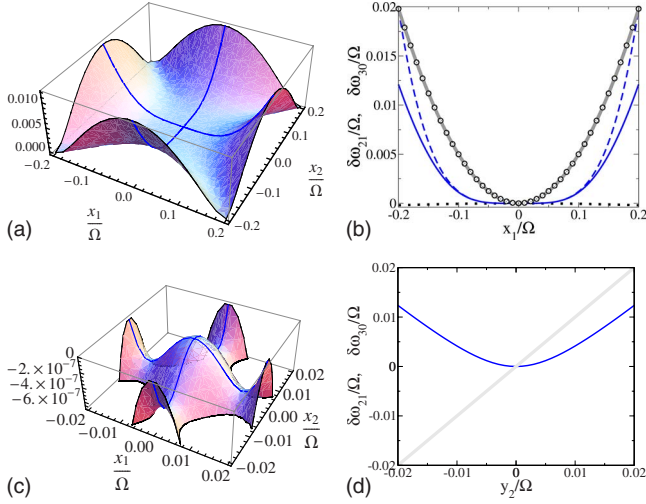
FIG. 1. (Color online) Dispersion of the SWAP and Z splittings for $\omega_c/\Omega = 0.01$. Left: $\delta\omega_{21}/\Omega$ from numerical diagonalization of $\mathcal{H}_0 + \mathcal{H}_I$ (top). Zoom around the origin highlights the interplay of second and fourth order terms, barrier height $\propto \omega_c^3$ (bottom). Right: comparative behavior of dispersions in the two subspaces. Top: SWAP exact splitting blue (gray) line, expansion (1) for $x_2 = 0$, $y_i = 0$ dashed blue (dashed gray), second order expansion (dotted), Z splitting (thick gray) $\delta\omega_{30} \simeq -\frac{\cos\varphi}{2}\{(y_1 + y_2) + [1 + \frac{1}{2}(\frac{\omega_c}{\Omega})^2]\frac{x_1^2 + x_2^2}{\Omega}\}$, and single-qubit dispersion (circles). Bottom: longitudinal dispersions. The Z subspace (light gray) is much more sensitive both to transverse and longitudinal variations.

with standard deviation $\Sigma_{ij} = \sqrt{\langle \delta\omega_{ij}^2 \rangle - \langle \delta\omega_{ij} \rangle^2}$, where $\delta\omega_{ij} = \omega_{ij}(\mathbf{X}) - \omega_{ij}$. The splittings enter the evolution of the reduced density matrix coherences in the eigenbasis of $\mathcal{H}_0$ as $\rho_{ij}(t) \approx \rho_{ij}(0)\int d\mathbf{X} P(\mathbf{X}) \exp[-i\omega_{ij}(\mathbf{X})t]$. The probability density can be taken of Gaussian form $P(X_\alpha) = \exp[-X_\alpha^2/2\Sigma_{X_\alpha}^2]/\sqrt{2\pi}\Sigma_{X_\alpha}$ in relevant cases.[8] Optimal tuning of control parameters is achieved when the variance of the relevant instantaneous splittings, Σ_{ij}, is minimized. It results in the reduction of $\rho_{ij}(t)$ decay due to defocusing processes.

If $\omega_{ij}(\mathbf{X})$ is monotonic in a region $|X_\alpha| \leq 3\Sigma_{X_\alpha}$, $\Sigma_{ij}^2 \approx \Sigma_\alpha [\frac{\partial\omega_{ij}}{\partial X_\alpha}|_{X_\alpha = 0}]^2 \Sigma_{X_\alpha}^2$. The variance attains a minimum for vanishing differential dispersion. This is the case of single-qubit optimal points. For the charge-phase two-port architecture, control is via gate voltage, $q_x \equiv C_g V_g/(2e)$, and magnetic flux dependent phase δ, entering the Josephson energy $E_J = E_J^0 \cos\delta$. Thus, $X_\alpha \to \Delta q_x$, ΔE_J and the optimal point, $q_x = 1/2$, $\delta = 0$, is at the saddle point of the energy bands.[2] When bands are nonmonotonic in the control parameters, minimization of defocusing necessarily requires their tuning to values depending on the noise variances. We illustrate potentialities of this result for a universal two-qubit gate.

$\sqrt{\text{i}-\text{SWAP}}$ *gate.* A simple way to realize two-qubit entanglement is via a fixed, capacitive or inductive, coupling scheme.[15] Fast two-qubit operations and coupling switching on/off are achieved by individual-qubit control. Fixed coupling has been used to demonstrate two-qubit logic gates[1(e),16] and high-fidelity Bell states generation in capacitive coupled phase qubits.[17]

The interaction is effectively switched on by tuning the single-qubit energy spacing to mutual resonance. The

building-block Hamiltonian reads $\mathcal{H}_0 = -\frac{\Omega}{2}\sigma_3^{(1)} \otimes \mathbb{1}^{(2)} - \frac{\Omega}{2}\mathbb{1}^{(1)} \otimes \sigma_3^{(2)} + \frac{\omega_c}{2}\sigma_1^{(1)} \otimes \sigma_1^{(2)}$ ($\hbar = 1$, $\sigma_3^{(\alpha)}|\pm\rangle = \pm|\pm\rangle$). The Hilbert space factorizes in a "SWAP subspace," spanned by the eigenstates of $\mathcal{H}_0$ $\{|1\rangle = \frac{1}{\sqrt{2}}(-|+-\rangle + |-+\rangle)$ and $|2\rangle = \frac{1}{\sqrt{2}}(|+-\rangle + |-+\rangle)\}$ (eigenvalues $\omega_{\frac{1}{2}} = \mp \omega_c/2$), and in a "Z subspace" generated by the eigenstates $\{|0\rangle = -\sin\frac{\varphi}{2}|++\rangle + \cos\frac{\varphi}{2}|--\rangle$ and $|3\rangle = \cos\frac{\varphi}{2}|++\rangle + \sin\frac{\varphi}{2}|--\rangle\}$, where $\tan\varphi = -\omega_c/(2\Omega)$ [eigenvalues $\omega_{\frac{0}{3}} = \mp \sqrt{\Omega^2 + (\omega_c/2)^2}$]. We focus on the $\sqrt{\text{i}-\text{SWAP}}$ operation $|+-\rangle \to |\psi_e\rangle = [|+-\rangle - i|-+\rangle]/\sqrt{2}$, which generates by free evolution an entangled state at $t_E = \pi/2\omega_c$. We consider the general case where $\mathcal{H}_I = -\frac{1}{2}[\hat{x}_1\sigma_1^{(1)} + \hat{z}_1\sigma_3^{(1)}] \otimes \mathbb{1}_2 - \frac{1}{2}\mathbb{1}_1 \otimes [\hat{x}_2\sigma_1^{(2)} + \hat{z}_2\sigma_3^{(2)}]$. Since transverse ($\hat{x}_i$) and longitudinal ($\hat{z}_i$) fluctuations usually have different physical origin, we assume they are independent.[18] For capacitive coupled charge-phase qubits, polarization fluctuations cause transverse noise $x_i \propto 4E_{C,i}\Delta q_{x,i}$ ($E_{C,i}$ qubit i charging energy), phase fluctuations lead to longitudinal noise $z_i \propto \Delta E_{J,i}$.[19] Both low-frequency fluctuations induce a stochastic effective SWAP splitting, $\omega_{21}(\{x_i, z_i\})$, the relevant scale for the gate operation. It can be obtained from $\mathcal{H}_0 + \mathcal{H}_I$ treating perturbatively the stochastic fields in $\mathcal{H}_I$,

$$\omega_{21}(x_1, x_2, z_1, z_2) \approx \omega_c - \frac{\omega_c}{2\Omega^2}(x_1^2 + x_2^2) + \frac{1}{2\omega_c}(z_1 - z_2)^2$$
$$+ \frac{\omega_c}{2\Omega^3}(x_1^2 + x_2^2)(z_1 + z_2) + \frac{1}{2\omega_c\Omega}(x_1^2 - x_2^2)$$
$$\times (z_1 - z_2) + \frac{\omega_c}{8\Omega^4}\left(1 + \frac{\omega_c^2}{\Omega^2}\right)$$
$$\times (x_1^4 + 6x_1^2 x_2^2 + x_2^4) + \frac{1}{8\omega_c\Omega^2}(x_1^2 - x_2^2)^2.$$

(1)

A key feature is that ω_{21} is nonmonotonic in the small coupling $\omega_c \ll \Omega$. This is due to a selection rule for longitudinal fluctuations. They only mix states inside each—SWAP or Z—subspace, while x_i fluctuations mix the two subspaces. For instance, second order transverse corrections to ω_1 are $\Sigma_{i\neq 1,2}|\langle 1|\mathcal{H}_I|i\rangle|^2/(\omega_1 - \omega_i) \propto \omega_c$, whereas longitudinal ones vary as $\omega_c^{-1} \propto |\langle 1|\mathcal{H}_I|2\rangle|^2/(\omega_1 - \omega_2)$. Nonmonotonicity in ω_c results in a competition between second and fourth order x_i terms in Eq. (1) and in nonmonotonic band structure, Fig. 1 (left). Because of this subtle feature, identification of the best operating condition necessarily requires consideration of the noise characteristics. Indeed, an *optimal coupling* can be found, which minimizes the SWAP variance

$$\Sigma_{21}^2 \approx \frac{1}{\omega_c^2}\left\{\left(\frac{\Sigma_x}{\Omega}\right)^4 [(\Sigma_x^2 - \omega_c^2)^2 + \Sigma_x^4 + \Sigma_{z_2}^2\Omega^2] + \frac{\Sigma_{z_2}^4}{2}\right\},$$

(2)

where we assumed equal transverse variances, $\Sigma_{x_i} = \Sigma_x$ and $\Sigma_{z_1} \ll \Sigma_{z_2}$, which mimic typical experimental conditions.[19] Equations (1) and (2) highlight the general result of this Brief Report. While higher stability with respect to *longitudinal* fluctuations is attained by larger couplings, minimiza-
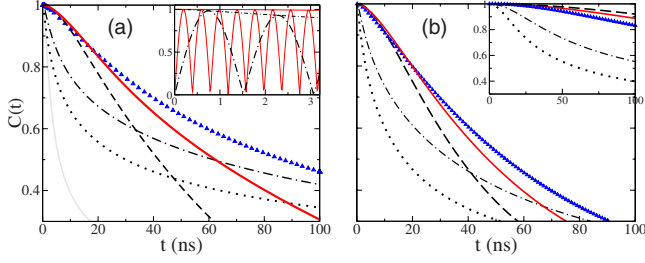
FIG. 2. (Color online) Envelope of the concurrence in the SPA, $\Omega=10^{11}$ rad/s. To elucidate the significance of the optimal coupling scheme, we consider $1/f$ amplitudes larger than expected from single-qubit measurements (Ref. 19). Left: effect of transverse noise with $\Sigma_x/\Omega=0.08$ and $\omega_c/\Omega=0.01, 0.02, 0.06, 0.08, 0.1$ (dotted, dot-dashed, triangles, thick (gray) red, dashed). Light gray is the single-qubit coherence, $|\rho_{+-}(t)|=[1+(\Sigma_x^2 t/\Omega^2)]^{-1/4}$ (Ref. 8). Inset: $C(t)$ and its envelope for $\omega_c/\Omega=0.02, 0.08$. For optimal coupling $\tilde{\omega}_c \approx \Sigma_x$, at 3 ns, already 8-SWAP cycles occurred. Right: effect of transverse plus longitudinal noise on qubit 2, $\Sigma_{z_2}/\Omega=2.5 \times 10^{-3}$. Inset: effect of longitudinal noise, ω_c values as in left panel.

tion of the detrimental *transverse* low-frequency noise components is obtained by tuning the coupling to an optimal value $\tilde{\omega}_c$. For $\Sigma_{z_2} \ll \Sigma_x$, this is the transverse noise variance, $\tilde{\omega}_c \approx 2^{1/4}\Sigma_x$. It can be estimated by independent measurement of the amplitude of the $1/f$ transverse noise on the uncoupled qubits, $S_x^{1/f}=\pi\Sigma_x^2[\ln(\gamma_M/\gamma_m)\omega]^{-1}$, $\Sigma_x^2=\int_0^\infty d\omega/\pi S_x^{1/f}(\omega)$ (low and high-frequency cutoffs γ_m and γ_M). Note the higher stability of the SWAP splitting compared to the qubits Larmor frequency and the Z splitting, Fig. 1.

Working at the optimal coupling minimizes defocusing and guarantees excellent performance of the $\sqrt{i-SWAP}$ operation. As an unambiguous test of entanglement generation and its degradation due to noise, we calculated the concurrence during the gate operation.[20] If the system is initialized in $|+-\rangle$, the 4×4 density matrix in the computational basis is nonvanishing only along the diagonal and anti-diagonal at any time (X states) and the concurrence takes a simple form.[21]
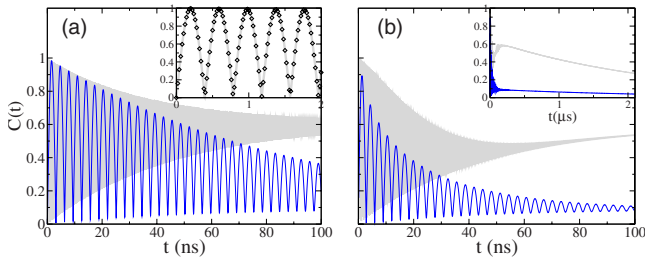

FIG. 3. (Color online) Concurrence for $\omega_c/\Omega=0.01$ blue (gray) line and for optimal coupling $\tilde{\omega}_c/\Omega=0.08$ (light gray). (a) Effect of high-frequency noise, $S_{x_i}(\omega)\approx8\times10^5$ s^{-1}, $S_{z_2}(\omega)\approx4\times10^7$ s^{-1} $\gg S_{z_1}(\omega_c=0.08\Omega)\approx6\times10^3$ s^{-1} (Ref. 23). Inset: at short times $C(t)\approx2|\text{Im}\{\rho_{12}(t)\}|$ (diamonds). (b) Effect of $1/f$ noise (parameters as in Fig. 2) and white quantum noise. Inset: asymptotic behavior. Results are minimally modified considering the dynamics of fluctuators generating $1/f$ transverse (longitudinal) noise in $\gamma_m=1$ s^{-1}, $\gamma_M=10^6(10^{10})$ s^{-1} (numerical solution of the stochastic Schrödinger equation).

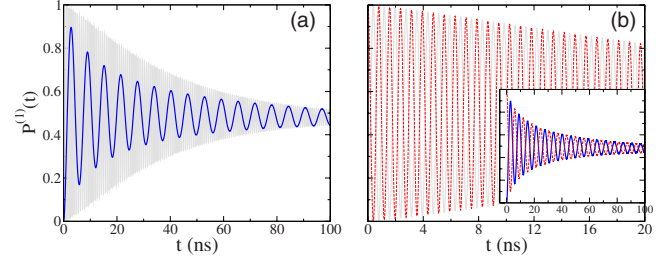

FIG. 4. (Color online) Qubit 1 switching probability to $|-\rangle$, $P^{(1)}(t)$, and probability $P^{(2)}(t)$ to find qubit 2 in the initial state $|-\rangle$ in the presence of $1/f$ and white noise for $\omega_c/\Omega=0.01$ blue (gray) line and for optimal coupling $\tilde{\omega}_c=\Sigma_x=0.08\Omega$ (light gray). (a) $P^{(1)}$: exponential short-time limit at $\tilde{\omega}_c$, algebraic otherwise. (b) $P^{(1)}$ and $P^{(2)}$ [dashed (gray) red] antiphase oscillations for $\tilde{\omega}_c$ (main), $\omega_c/\Omega=0.01$ (inset).

We first consider the effect of low-frequency fluctuations. In the adiabatic approximation, the concurrence simplifies to $C(t)=2|\text{Im}\{\rho_{12}(t)\}|$. With the SWAP-splitting expansion (1) (including in the third and fourth order the terms $\propto\omega_c^{-1}$) in the SPA, we obtain

$$\rho_{12}(t)=\rho_{12}(0)\frac{\Omega}{2\Sigma_x^2}\sqrt{\frac{2i\omega_c}{\pi t}}e^{i\omega_c t+h(t)}K_0[h(t)], \quad (3)$$

where $h(t)=(\Sigma_{z_1}^2+\Sigma_{z_2}^2+i\omega_c/t)(\Omega^2/\Sigma_x^2+i\omega_c t)^2/(4\Omega^2)$, and $K_0[h]$ is the K-Bessel function of order zero.[22] By increasing the coupling to match the optimal condition, two goals are simultaneously achieved: minimization of initial defocusing and fast two-qubit gate (Fig. 2). The first SWAP error takes remarkable values $\varepsilon=1-\langle\psi_e|\rho(t_E)|\psi_e\rangle\approx10^{-3}-10^{-4}$, for $\omega_c\approx\Sigma_x\leq0.05\Omega$ (numerical simulations). This is an interesting effect, considering that single-qubit coherence times would be rather small at the same $1/f$ amplitudes, $T_2\approx5$ ns. The optimal coupling scheme is effective against large amplitude $1/f$—noise even in the presence of high-frequency fluctuations. Within the secular approximation, quantum noise leads to additional exponential decay of SWAP-coherence, $\tilde{\rho}_{12}(t)=\rho_{12}(t)\exp\{-\tilde{\Gamma}_{12}t\}$. Thermal relaxation processes ($k_BT\ll\Omega$) populate levels $i=0-2$ and the concurrence reads $C(t)\approx\sqrt{(\rho_{11}-\rho_{22})^2+2(\text{Im}[\tilde{\rho}_{12}])^2}-|\sin\varphi|\rho_{00}$. The SWAP decay rate is related to escape rates from levels 1 and 2, $\tilde{\Gamma}_{12}\approx\frac{\Gamma_1^e+\Gamma_2^e}{2}$, where $\Gamma_1^e=\Gamma_{10}+\Gamma_{12}$, $\Gamma_2^e=\Gamma_{20}+\Gamma_{21}$ and $\Gamma_{i0}\propto[S_{x_1}(\omega_{i0})+S_{x_2}(\omega_{i0})]$, $\Gamma_{21}\propto[S_{z_1}(\omega_{21})+S_{z_2}(\omega_{21})]$.

These rates enter the populations in the combinations $\Gamma_\pm=-(\Gamma_1^e+\Gamma_2^e)/2\pm\sqrt{(\Gamma_1^e-\Gamma_2^e)^2+4\Gamma_{12}\Gamma_{21}}/2$.[23] The SWAP-coherence rules the relevant short-time behavior, $|\rho_{12}|\propto1-\tilde{\Gamma}_{12}t$ [or $|\rho_{12}|\propto1-(\Sigma_{21}t)^2/2$] depending on the most relevant quantum (or adiabatic) noise component. Exponential decay is due to the strongest longitudinal or transverse quantum noise, Fig. 3. The finite asymptotic value reflects the entangled thermalized state (no "entanglement sudden death" occurs).[21] The above entanglement characterization translates into directly measurable quantities. Out of phase oscillations of single-qubit switching probabilities signals two-qubit states anticorrelations.[17] It follows from $P^{(\frac{1}{2})}(t)$

$= P(t) \pm \mathrm{Re}[\rho_{12}(t)]$, with $P(t) = -\frac{1}{2}\cos\varphi[\rho_{11}(t) + \rho_{22}(t)] + \cos^2(\frac{\varphi}{2})$. For a charge-phase $\sqrt{\mathrm{i} - \mathrm{SWAP}}$ gate,[13] defocusing due to $1/f$ polarization and phase noise is considerably reduced at optimal coupling, Fig. 4. Phase quantum noise on qubit 2 displaced by its optimal point contributes to initial decay. Oscillations visibility is larger than 90% until ≈ 10 ns, corresponding to ≈ 25 SWAP cycles. This contrasts with strong initial decay for nonoptimal coupling. Long-time exponential decay is due to polarization quantum noise.

In conclusion, we have proposed a general route to reduce inhomogeneities due to $1/f$ noise by exploiting tunability of nanodevices. As a relevant and timely issue, we have illustrated the considerable improvement of the entangled dynamics in a universal two-qubit gate. It requires preliminary noise characterization and work in the protected SWAP-subspace. In the considered scheme, coupling is controllable by dynamically tuning the qubit frequencies. We demonstrated that an efficient gate may be obtained with no additional dynamical decoupling protocols, even if at least one qubit has to be moved away from its own optimal point. In order to implement a scalable architecture, this scheme has to be supplemented by switchable coupling between small subunits, formed by single-qubit and universal two-qubit gates.[12] Note that our approach can also be applied to directly switchable coupling schemes which have been recently proposed as alternative, potentially scalable, designs.[24,25]

In the broader perspective of fault tolerant architectures in the solid state, our work provides a strong hint on how to extend the analysis of Ref. 11 to include the effect of time-correlated phase errors, typically affecting nanodevices. Note, in this respect, that fixed coupling schemes are at the basis of qubit encoding.[11]

Finally, we remark that the device reliability may be qualified by the impact of one/few impurities strongly coupled to it.[8,26] These induce non-Gaussian fluctuations which randomly displace qubits from resonant condition, possibly resulting in limited readout fidelity.[13] These effects are neglected the present analysis, but could be addressed as suggested in Ref. 8.

[1] Y. Nakamura *et al.*, Nature (London) **398**, 786 (1999); Y. Yu *et al.*, Science **296**, 889 (2002); J. M. Martinis *et al.*, Phys. Rev. Lett. **89**, 117901 (2002); I. Chiorescu *et al.*, Science **299**, 1869 (2003); T. Yamamoto *et al.*, Nature (London) **425**, 941 (2003); S. Saito *et al.*, Phys. Rev. Lett. **93**, 037001 (2004); J. Johansson *et al.*, *ibid.* **96**, 127006 (2006); F. Deppe *et al.*, Nat. Phys. **4**, 686 (2008); J. A. Schreier *et al.*, Phys. Rev. B **77**, 180502(R) (2008).

[2] D. Vion *et al.*, Science **296**, 886 (2002); G. Ithier *et al.*, Phys. Rev. B **72**, 134519 (2005).

[3] S. Poletto *et al.*, New J. Phys. **11**, 013009 (2009).

[4] M. Mück *et al.*, Appl. Phys. Lett. **86**, 012510 (2005); J. Eroms *et al.*, *ibid.* **89**, 122516 (2006).

[5] Y. Nakamura *et al.*, Phys. Rev. Lett. **88**, 047901 (2002).

[6] E. Paladino *et al.*, Phys. Rev. Lett. **88**, 228304 (2002).

[7] C. P. Schlichter, *Principles of Magnetic Resonance* (Springer, New York, 1996).

[8] G. Falci *et al.*, Phys. Rev. Lett. **94**, 167002 (2005).

[9] L. Vandersypen and I. Chuang, Rev. Mod. Phys. **76**, 1037 (2005).

[10] F. Yoshihara *et al.*, Phys. Rev. Lett. **97**, 167001 (2006).

[11] E. Knill, Nature (London) **434**, 39 (2005).

[12] M. Nielsen and I. Chuang, *Quantum Computation and Quantum Information* (Cambridge University Press, Cambridge, England, 2005).

[13] F. Nguyen, Thesis, Paris 6 University, 2008.

[14] O. Astafiev *et al.*, Phys. Rev. Lett. **93**, 267007 (2004).

[15] Yu. Makhlin *et al.*, Nature (London) **398**, 305 (1999); J. Q. You *et al.*, Phys. Rev. Lett. **89**, 197902 (2002); E. Ferraro, M. Scala, R. Migliore, A. Napoli, Phys. Rev. A **80**, 042112 (2009).

[16] Yu. A. Pashkin *et al.*, Nature (London) **421**, 823 (2003); A. J. Berkley *et al.*, Science **300**, 1548 (2003); J. B. Majer *et al.*, Phys. Rev. Lett. **94**, 090501 (2005); J. H. Plantenberg *et al.*, Nature (London) **447**, 836 (2007).

[17] R. McDermott *et al.*, Science **307**, 1299 (2005); M. Steffen *et al.*, *ibid.* **313**, 1423 (2006).

[18] Correlated noise and cross-talk effects have been addressed in A. D'Arrigo *et al.*, New J. Phys. **10**, 115006 (2008).

[19] Working point $q_{i,x} = 1/2$, $\delta_1 = 0$, resonance is achieved tuning $\delta_2 \approx 0.45$ (Ref. 13). Noise figures are extrapolated from single-qubit data (Ref. 2). Since for both qubits $q_{i,x} = 1/2$, $\Sigma_{x,i} = \Sigma_x \approx 0.02\Omega$. $\Sigma_{z_2} \approx 8 \times 10^{-4}\Omega$, phase noise on qubit 1 operating at $\delta_1 = 0$ is negligible, $\Sigma_{z_1}/\Omega \approx 10^{-5}$.

[20] W. K. Wooters, Phys. Rev. Lett. **80**, 2245 (1998).

[21] T. Yu and J. H. Eberly, Phys. Rev. Lett. **97**, 140403 (2006).

[22] M. Abramowitz and I. A. Stegun, *Handbook of Mathematical Functions* (Dover, New York, 1965).

[23] E. Paladino *et al.*, Physica E **42**, 439 (2010).

[24] D. V. Averin and C. Bruder, Phys. Rev. Lett. **91**, 057003 (2003); Alexandre Blais *et al.*, *ibid.* **90**, 127901 (2003); F. Plastina and G. Falci, Phys. Rev. B **67**, 224514 (2003); C. Rigetti *et al.*, Phys. Rev. Lett. **94**, 240502 (2005); Yu-xi Liu *et al.*, *ibid.* **96**, 067003 (2006).

[25] T. Hime *et al.*, Science **314**, 1427 (2006); A. O. Niskanen *et al.*, *ibid.* **316**, 723 (2007); Mika A. Sillanpää *et al.*, Nature (London) **449**, 438 (2007); J. Majer *et al.*, *ibid.* **449**, 443 (2007); S. H. W. van der Ploeg *et al.*, Phys. Rev. Lett. **98**, 057004 (2007); A. Fay *et al.*, *ibid.* **100**, 187003 (2008).

[26] Y. M. Galperin *et al.*, Phys. Rev. Lett. **96**, 097009 (2006).